RESEARCH ARTICLE

Small proline-rich repeat 3 is a novel coordinator of PDGFRβ and integrin β1 crosstalk to augment proliferation and matrix synthesis by cardiac fibroblasts

Sarika Saraswati[1] 🆔 | Caressa D. Lietman[1] | Bin Li[1] | Sijo Mathew[2] | Roy Zent[3] | Pampee P. Young[1,4]

[1]Department of Pathology, Microbiology, and Immunology, Vanderbilt University Medical Center, Nashville, TN, USA

[2]Department of Pharmaceutical Sciences, School of Pharmacy, North Dakota State University, Fargo, ND, USA

[3]Division of Nephrology and Hypertension, Department of Medicine, Vanderbilt University Medical Center, Nashville, TN, USA

[4]American Red Cross, Biomedical Division, Washington, DC, USA

Correspondence
Pampee P. Young, Department of Pathology, Microbiology, and Immunology, Vanderbilt University Medical Center, 1161 21st Avenue South, MCN C2217, Nashville, TN 37232, USA.
Email: pampee.young@redcross.org

Sarika Saraswati, Department of Pathology, Microbiology, and Immunology, Vanderbilt University Medical Center, 1161 21st Avenue Soutn, MCN C2217, Nashville, TN, 37232, USA.
Email: sarika.saraswati@vanderbilt.edu and sarika.saraswati@vumc.org

Abstract

Nearly 6 million Americans suffer from heart failure. Increased fibrosis contributes to functional decline of the heart that leads to heart failure. Previously, we identified a mechanosensitive protein, small proline-rich repeat 3 (SPRR3), in vascular smooth muscle cells of atheromas. In this study, we demonstrate SPRR3 expression in cardiac fibroblasts which is induced in activated fibroblasts following pressure-induced heart failure. *Sprr3* deletion in mice showed preserved cardiac function and reduced interstitial fibrosis in vivo and reduced fibroblast proliferation and collagen expression in vitro. SPRR3 loss resulted in reduced activation of Akt, FAK, ERK, and p38 signaling pathways, which are coordinately regulated by integrins and growth factors. SPRR3 deletion did not impede integrin-associated functions including cell adhesion, migration, or contraction. SPRR3 loss resulted in reduced activation of PDGFRβ in fibroblasts. This was not due to the reduced PDGFRβ expression levels or decreased binding of the PDGF ligand to PDGFRβ. SPRR3 facilitated the association of integrin β1 with PDGFRβ and subsequently fibroblast proliferation, suggesting a role in PDGFRβ-Integrin synergy. We postulate that SPRR3 may function as a conduit for the coordinated activation of PDGFRβ by integrin β1, leading to augmentation of fibroblast proliferation and matrix synthesis downstream of biomechanical and growth factor signals.

Abbreviations: CF, cardiac fibroblast; DMEM, Dulbecco's modified eagle medium; ECM, extracellular matrix; HBSS, Hank's balanced salt solution; HEPES, (4-(2-hydroxyethyl)-1-piperazineethanesulfonic acid; HF, heart failure; IVS, interventricular septum; KO, knock out; LVID, left ventricular internal diameter; LVPW, left ventricular posterior wall; PCR, polymerase chain reaction; PDGFBB, platelet-derived growth factor-BB; SPRR3, small proline-rich repeat 3; TAC, transverse aortic constriction; TUNEL, terminal deoxynucleotidyl transferase dUTP nick end labeling; WT, wild-type; VSMCs, vascular smooth muscle cells.

Sarika Saraswati and Caressa D. Lietman contributed equally to the work.

1 | INTRODUCTION

Heart failure is a major cause of death worldwide and is associated with progressive interstitial fibrosis.[1] The normal adult heart is comprised of many cell types, including cardiac fibroblasts (CFs) that account for about 20%-30% of the total cardiac cell population.[2,3] Under normal conditions, CFs maintain a quiescent state in both the interstitium and surrounding blood vessels.[4] Fibroblasts play a central role in the heart's response to injury by regulating matrix synthesis and deposition, and other aspects of repair, including angiogenesis.[5] Following injury or with aging, activation and proliferation of cardiac fibroblasts leads to excess matrix deposition and scarring. Pathophysiological stressors such as hypertension lead to increased fibrosis, myocyte loss and uncoupling, and eventual heart failure.[6,7]

Our understanding of the molecular players regulating pressure and volume overload-induced changes in cardiac fibroblasts is incomplete.[8] During both pressure and volume overload, myocytes and fibroblasts undergo strain, causing the transduction of intracellular signals via integrins.[9] Integrin receptors are critical in linking the extracellular matrix (ECM) to the cytoskeleton and in modulating intracellular signaling in response to biomechanical changes in the ECM.[10] Integrin β1 and its activation of FAK are involved in pressure-overload mediated fibrosis.[11] Additionally, after pressure overload, isolated cardiac fibroblasts display changes in adhesion, migration, and collagen gel contraction, which are all dependent on integrin β1 activity.[8] Integrins can modulate intracellular signaling directly or coordinately with many growth factor receptors, including epidermal growth factor receptors (EGFR), insulin receptor, and platelet derived growth factor receptor (PDGFR).[10,12-15] In fact, positive crosstalk allows integrins to amplify growth factor receptor signaling by either receptor phosphorylation or direct physical interaction.[10,12-15] The mechanisms of this synergistic signaling vary among the various integrin-growth factor receptor pairs and are incompletely understood.

Small proline-rich repeat protein 3 (SPRR3) is a member of the SPRR family, which is known to be expressed abundantly in the foregut and esophagus.[16,17] Our group identified that SPRR3 is upregulated exclusively in vascular smooth muscle cells (VSMCs) of the atheromas of large arteries.[18] SPRR3 is not expressed otherwise in the VSMCs of arteries, veins, or capillaries.[18] SPRR3 expression, in the VSMCs of atheromas, is induced in response to mechanic cyclic stress, which is sensed through the presence of integrin α1β1, a major receptor for collagen.[19] SPRR3 regulates VSMC proliferation and type I collagen production in a PI3/Akt-dependent manner. We previously demonstrated that SPRR3 also regulates p38 activation in VSMCs[20,21]; findings that were confirmed by others in breast and colorectal cancer.[22,23] However, the molecular mechanisms by which SPRR3 regulates diverse downstream signaling pathways is unknown.

In this study, we report that *Sprr3* within the heart is expressed by cardiac fibroblasts. In order to elucidate the role of *Sprr3* in fibroblasts and their response to pathologic stress, we performed transverse aortic constriction (TAC) in *Sprr3*^{−/−} mice to induce pressure overload heart failure.[5] *Sprr3* ablation conferred resistance to pressure overload heart failure and reduced fibrosis. We evaluated the mechanism by which SPRR3 augments fibrosis by evaluating its role on fibroblast number and function. Interestingly, our data point to a role of SPRR3 in activation of multiple and diverse signaling pathways, including FAK, ERK, and p38, likely by facilitating PDGFRβ/ integrin β1 crosstalk, and thereby modulating cellular effects downstream.

2 | MATERIALS AND METHODS

2.1 | Animal model

All procedures were carried out in accordance with the recommendations in the Guide for the Care and Use of Laboratory Animals of the National Institutes of Health and Vanderbilt Institutional Animal Care and Use Committee (Protocol number: V/17/004). *Sprr3*^{−/−} mice were generated and maintained by PPY on a C57Bl/6J background as previously reported.[21] C57Bl/6J mice were purchased from the Jackson Laboratory (Bar Harbor, ME). Only male mice were used for the study. Mice received TAC surgery using 22-gauge needles at 3 months of age. Mice were anesthetized with ketamine (120 mg/kg) and Xylazine (10 mg/kg) by intra-peritoneal injection prior to surgery. The analgesic buprenorphine (0.1 mg/kg) was administered intra-peritoneally at the time of surgery and every 8-12 hours for up to 72 hours following surgery. For echocardiography, cardiac dimensions were obtained from 2-D Guided M-mode images (100 frames/sec) and were read blinded using short axis and parasternal long-axis views. All measurements were done on un-sedated mice at day 7 and day 60 post TAC. Measurements were averaged over 3 consecutive beats from the LV posterior wall (LVPW),

the interventricular septum (IVS), and LV internal diameter (LVID). After day 60, mice were euthanized via isoflurane overdose and hearts were excised for subsequent experiments.

2.2 | Cell culture

Primary mouse cardiac fibroblasts were isolated from mice hearts by the previously described protocol.[24] Briefly, heart tissue was minced and placed into Krebs-Henseleit (K3753a; Sigma-Aldrich, St. Louis, MO, USA) buffer with 2.9 mM of $CaCl_2$ and 24 mM of $NaHCO_3$ containing a cocktail of 0.25 mg/mL Liberase TH (5401151001; Sigma-Aldrich), 20 U/mL DNase I (7326828; Bio-Rad, Hercules, California, USA), 10 mM of HEPES (15630080; Thermo Fisher Scientific, Waltham, MA, USA) in Hank's balanced salt solution (HBSS; MT21020CV, Thermo Fisher Scientific) and shaken at 37°C for 20 minutes. Cells collected after digestion were passed through a 40 μm nylon mesh and centrifuged (15 minutes, 200 g, 4°C). Finally, cells were reconstituted with DMEM-F12 medium (11320033; Thermo Fisher Scientific) containing 10% of FBS (PS-FB1; Peak Serum, Wellington, Colorado, USA) and 1% of Penicillin/Streptomycin (15140122; Thermo Fisher Scientific) and seeded onto plastic plates (CLS430167; Sigma-Aldrich) for separation of fibroblasts by selective adhesion for 4 hours at 37°C. Mouse embryonic fibroblasts were isolated from E13.5 embryos. The heads and organs were removed, and the remaining tissue was minced and digested using trypsin for 15 minutes at 37°C. The cells were resuspended in DMEM supplemented with 10% of FBS and 1% of penicillin/streptomycin. Fibroblasts were isolated by selective adhesion.

2.3 | Immunoprecipitation

Immunoprecipitation (IP) experiments were performed using the Pierce Crosslink Immunoprecipitation Kit (26147; Thermo Fisher Scientific) per manufacturer's directions. Briefly, 8 μg of antibody were coupled to Pierce Protein A/G Plus Agarose beads and crosslinked by DSS crosslinker. *Sprr3*$^{-/-}$ smooth muscle cells overexpressing either GFP or SPRR3 were lysed, and 2 mg of lysate was precleared using Control Agarose Resin for 1 hour. The cleared lysate was then incubated with the antibody-crosslinked beads overnight at 4°C, and eluted. Analysis was performed by Western Blot.

2.4 | In situ proximity ligation

These assays were performed using the Duolink PLA Protein Detection Technology with the Duolink Starter Orange Kit

Goat/Rabbit (DUO92106; Sigma Aldrich) per the manufacturer's directions. Fibroblasts were seeded at 25 000 cells/well on 8-well chamber slides overnight. They were fixed with acetone for 15 minutes then washed with PBS. Slides were blocked with 10% of donkey serum in blocking buffer for 30 minutes at 37°C. Primary antibodies were diluted in 3% of donkey serum in blocking buffer overnight in a humidity chamber at 4°C. The PLA Probes (PLUS and MINUS) were diluted 1:5 in Antibody Diluent for 1 hour at 37°C then washed. Ligation Ligase solution was diluted 1:5 in water and incubated at 37°C for 30 minutes then washed. Amplification-Polymerase solution diluted 1:5 in water was used for 100 minutes at 37°C and washed. Slides were mounted with Duolink in Situ Mounting Medium with DAPI (DUO82040; Sigma Aldrich).

2.5 | RNA isolation and semi quantitative PCR

RNA was isolated from cells using Trizol (15596026; Thermo Fisher Scientific) following the manufacturer's protocol. First strand DNA synthesis was performed with 1 μg RNA using the iScript cDNA synthesis kit (170-8890; Bio-Rad). Semi quantitative real-time PCR (RT-PCR) was performed in triplicate for each sample with iCycler (Bio-Rad) and fluorescent detection (172-5200; SsoFast EvaGreen; BioRad). Each reaction was normalized against 18S. Primer sequences are as shown in Table 1.

2.6 | Immunoblotting

For protein collection, cultured cells were serum starved for 4 hours in DMEM, then, were washed twice with PBS and lysed using RIPA buffer supplemented with protease inhibitors (04693159001; Sigma Aldrich) and phosphatase inhibitors (P0759 and P0758; New England Biolabs, Ipswich, MA, USA). Whole cell lysates were rocked 30 minutes at 4°C then spun 15 minutes at 13 000 *g* and the supernatant collected. Protein concentrations were determined using a bicinchoninic acid (BCA) Protein Assay Kit (23225; Thermo Fisher Scientific). Proteins were denatured 10 minutes at 95°C in SDS sample buffer before being resolved by SDS-PAGE electrophoresis and transferred onto a nitrocellulose membrane (NBA083C001EA; PerkinElmer, Waltham, MA, USA). In some experiments, premade tissue blots with protein extracts from multiple species (human, rat, and mouse) were commercially purchased (TB35 and TB71; GBiosciences, St. Louis, MO). Blots were blocked in 5% of nonfat milk and probed with antibodies overnight at 4°C. After washing with 0.1% of Tween-20-supplemented TBS, blots were incubated with species-specific secondary antibodies for 1 hour at room

TABLE 1 Primers used to analyze the gene expression changes by semi-quantitative real time PCR analysis

Gene	Forward	Reverse
Col1a1	5′-GCC AGA TGG GTC CCC GAG GT-3′	5′-GGG GGT CCA GCA GCA CCA AC-3′
Sprr3	5′-CCC TTT GTC CCA CTC CT-3′	5′-TTG GTG TTT CCT GGT TGT G-3′
cTnT	5′-GAG ACA GAC AGA GAG AGA GAA-3′	5′-TGC TGC TTG AAC TTT TCC TGC-3′
Fsp1	5′-CGG TTA CCA TGG CAA GAC CC-3′	5′-TGT GCG AAG CCA GAG TAA G-3′
CD31	5′-GTG AAG GTG CAT GGC GTA TC-3′	5′-CAC AAA GTT CTC GTT GGA GGT-3′
Postn	5′-TGC TGC CCT GGC TAT ATG-3′	5′-GTA GTG GCT CCC ACA ATG-3′
NG2/AN2	5′-CCT CAG AGC CCT ATC TCC ACG TAG C-3′	5′-CAT CAC CAA GTA GCC AGC GTT CG-3′
18S	5′-CGC CGC TAG AGG TGA AAT TCT-3′	5′-CGA ACC TCC GAC TTT CGT TCT-3′

temperature and chemiluminescence (NEL104; PerkinElmer) was detected by film or visualized using a Syngene GBox (Syngene, Cambridge, United Kingdom). Image Studio Lite Ver 5.2 (LI-COR; Lincoln, Nebraska, USA) was used for densitometry analysis of the appropriate lanes; values are normalized to β-actin or GAPDH loading control.

2.7 | Transient transfection

FuGene HD (E2311; Promega, Madison, WI, USA) was used per the manufacturer's directions. MEFs were plated at 100 000 cells/well on a 6-well plate overnight. About 2 ug of total DNA was mixed up to 100 μL of PBS and 7 μL of FuGene HD. After a 15-minute incubation, the mixture was added dropwise to cells. Cells were collected 72 hours after transfection.

2.8 | Cell treatments

Ly294002 (Sigma Aldrich) was used as a PI3K inhibitor at a concentration of 25 μM for 1 hour. MK-2206 (2.5 μM, Selleck Chemicals, Houston, TX, USA) was used as a second Akt inhibitor. SC79 (10 μM, Sigma Aldrich) was used as an Akt activator for 24 hours. PDGFBB (PMG0041; Thermo Fisher Scientific) was used at 10 ng/mL concentration in DMEM without serum for the indicated times. Plates or chamber slides were coated with fibronectin at 1 ng/mL concentration overnight in PBS. They were then blocked in 0.5% of heat-inactivated BSA at 37° for 30 minutes before cells were plated.

2.9 | Flow cytometry

About 250 000 cells per sample were spun into a 96-well plate. They were resuspended in 200 μL DMEM Fluorobrite media (A1896701; Thermo Fisher Scientific)—for active integrin β1 1.8 mM of $CaCl_2$ and 1 mM of $MgCl_2$ were added

to the media to stabilize the conformation—with the appropriate antibodies (integrin β1 1:50; Active β1 9EG7 1:2000) for 1 hour. They were washed in media then incubated with secondary antibodies conjugated to fluorophores (Anti-rat Alexa 405; ab175670; 1:100; Abcam, Cambridge, MA, USA) for 30 minutes then washed. Gating was set using unlabeled controls, IgG controls (Rat IgG2, kappa monoclonal; ab18450; Abcam), and secondary only controls. All samples were analyzed using a Becton Dickinson (BD) Special Order Research Product (SORP) LSR Fortessa equipped with lasers at the following wavelengths: 405, 488, 561, and 640 nm. Samples were acquired using BD FACSDiva v 8.1.

2.10 | Collagen gel contraction

Mouse embryonic fibroblasts were resuspended to 3.3×10^6 cells/mL in serum-free DMEM. To coat the wells, collagen (4.1 mg/mL), HEPES (1 M), $NaHCO_3$ (0.37 G/5 mL water), and 2X DMEM were combined. The mixture was combined with cells to a 1:10 dilution. About 300 μL of solution were placed per well in a 48-well plate (total 100 000 cells/well). After incubating for 20 minutes at 37°C, the gel was released from the edges with a 30 G needle. About 600 μL of DMEM + 10% of FBS was added and images were taken every 24 hours. Contraction was quantified using ImageJ.

2.11 | Migration

Cell migration was measured using Boyden's Chamber Assay. Filters were coated with fibronectin at 1:50 dilution in PBS for 30 minutes at 37°C, then, blocked with 1% of BSA in PBS overnight. Cells were serum starved overnight. Fibroblasts were diluted to 10 000 cells/100 μL in DMEM + 1% of FBS. Stimulus was placed in the wells, while cells were added to the top of the transwell inserts. Cells were fixed with 10% of formalin for 30 minutes then stained with 0.5% of Crystal Violet/0.2 M of Boric Acid for 30 minutes at room temperature. The transwells

were destained with water and cells on the upper side of the well were removed with a cotton swab. The bottom of the transwell was imaged and quantified using CellSens.

2.12 | Cell adhesion

A 96-well plate was coated with fibronectin (serially diluted from 10 to 0.01 μg/mL) or 100% of FBS overnight at 4°C. Wells were then blocked with 0.5% of heat-denatured BSA for 30 minutes at 37°C. Cells were serum starved overnight, then, diluted to 10 000 cells/200 μL and added to the plate, then, incubated for 15-60 minutes. Wells were washed with PBS + 1 mM of CaCl$_2$ and 1 mM of MgCl$_2$, then, fixed in methanol for 10 minutes. They were stained with 0.5% of crystal violet/0.2 M of Boric acid for 10 minutes. After washing, methanol was used to recover the stain from the cells, and the plate was measured with a spectrophotometer at 595 nm.

2.13 | Histology and morphometry

Hearts were fixed in 10% of buffered formalin for 24 hours, embedded in paraffin and sectioned into 5 μm transverse sections. H&E and Masson's Trichrome staining was performed by the Vanderbilt Translational Pathology Shared Resource. Olympus DP71 microscope camera (Olympus America, Center Valley, PA) was used for imaging H&E and Masson's Trichrome stained sections. For immunofluorescence staining, slides were deparaffinized and hydrated through xylene and ethanol steps. Heat-mediated antigen retrieval was performed by boiling in citrate buffer (pH 6). Cells seeded onto coverslips were fixed for 1 hour at room temperature in 1% of paraformaldehyde, permeabilized with 0.1% of Triton-X in 0.1% of sodium citrate for 2 minutes on ice and washed several times with PBS. Following blocking with 10% of goat serum in 1% of BSA solution for 1 hour at room temperature, sections were incubated with primary antibody at 4°C overnight, and Alexa Fluor 488 or Cy3 conjugated secondary antibodies at room temperature for 1 hour. The slides were then counterstained with Hoechst 33342 (H21492; Invitrogen, Carlsbad, CA, USA) and mounted with Slowfade Gold (S36936; Life Technologies, Grand Island, NY, USA). For confocal microscopy, LSM510 (Zeiss) microscope was used to capture 1 μm optical slices.

2.14 | Proliferation

Primary fibroblasts were counted and seeded on 96-well plates. Following attachment onto plates, cells were serum starved for 24 hours. Then, cells were cultured in DMEM supplemented with 10% of FBS and antibiotics/fungizone for 24 hours. Cell number was determined using Fluorometric dsDNA quantitation kit (F2962; Thermo Fisher Scientific).

2.15 | BrdU proliferation assay

MEF proliferation was assessed by 5-bromo-2′-deoxyuridine (BrdU) cell proliferation assay (Calbiochem, Gibbstown, NJ, USA). WT and *Sprr3$^{-/-}$* MEFs were serum starved, then, plated on 1 μg/mL fibronectin coated plates in serum-free media for 24 hours. Cells were treated with/without 10 μg/mL integrin β1 antibody for 1 hour at 37°C prior to stimulation with PDGF for 15 and 30 minutes. BrdU incorporation was assessed by measured absorbance at dual wavelength of 450/595 nm following manufacture's protocol.

2.16 | Apoptosis (TUNEL) assay

For TUNEL staining, a 1:10 mix of enzyme: label diluted 5-fold with TUNEL dilution buffer (In Situ Cell Death Detection Kit TMR Red; 12156792910; Sigma Aldrich) was added to samples along with the secondary antibody and incubated for 60 minutes at 37°C. Samples were then counter stained with Hoechst and mounted as usual. Images were taken at 10×, 20×, or 40× magnification using an Axio Imager2 microscope (Carl Zeiss, Thornwood, NY, USA) and CoolSNAP HQ CCD camera (Photometrics, AZ, USA), and quantified using ImageJ.

2.17 | Antibodies

The following antibodies were used: Alpha Smooth Muscle Actin (α-SMA) (1:1000; Sigma A2547), Periostin (1:100; Santa Cruz, SC67233), collagen I (1:500; MD Bioproducts, #203002A), phospho-Akt (1:500; Cell Signaling, #4058S), Akt (1:500; Cell Signaling, #9272), pSmad2 (1:500; Cell Signaling, #3108S), Smad2/3 (1:500; Cell Signaling, #5678S), β-actin (1:5000; Sigma, #A5441), and SPRR3 (1:500; Proteintech group 11742-1-AP, or custom made) p-p38 (1:500; Cell Signaling), p38 (1:500; Cell Signaling), FAK (1:1000; Cell Signaling, #3285), p-FAK (1:500; Cell Signaling; #3283), GAPDH (1:500; Millipore; MAB374), p-PDGFRβ (Tyr751) (1:1000; Cell Signaling; #3161), PDGFRβ (28E1) (1:1000; Cell Signaling; #3169), integrin β1 (1:1000; R&D; #AF2405), total integrin β1 (flow cytometry, BD Pharmingen #550530), active integrin β1 (BD Pharmingen; #553715), and integrin β1 (Abcam; ab24693; 10 ug/ml for proliferation).

2.18 | Statistical analysis

The statistical significance between experimental and control groups were determined by One-way ANOVA with Bonferroni correction for multiple comparisons when multiple groups were compared. The D'Augustino and Pearson

omnibus or the Shapiro-Wilk tests were used to determine whether the data sets were normally distributed. For data sets that were not normally distributed or had N < 7, the Kruskal-Wallis H test was used instead of One-way ANOVA. For comparison between two groups of data, unpaired t test was used for normally distributed data sets, and Mann-Whitney test was used for data that were not normally distributed. GraphPad Prism (San Diego, CA) software was used for all statistical analyses. $P < .05$ was considered statistically significant in two-tailed hypothesis tests.

3 | RESULTS

3.1 | *Sprr3* is expressed in cardiac fibroblasts and cardiac *Sprr3* expression is regulated by stress in vivo

Previous work from our lab showed that *Sprr3* is undetectable in normal vasculature but is upregulated in vascular smooth muscle cells of atheroma.[19] We sought to identify other tissues that expressed *Sprr3*, apart from the esophagus, foregut, and atheromatous plaques, and found the expression of SPRR3 protein in tissue extracts from normal heart in human, rat, and mouse, but not in other tissues such as liver, lung kidney, brain or skeletal muscle (Figure 1A,B). As cardiomyocytes and cardiac fibroblasts are two significant cell populations in the heart, we isolated each population and assayed for *Sprr3* transcript expression. Cardiomyocytes, as indicated by the expression of myocyte-specific marker, *cTnt*, showed undetectable levels of *Sprr3* mRNA, whereas freshly isolated cardiac fibroblasts positive for *Col1a1* and *Fsp1*[25,26] were also positive for *Sprr3* mRNA (Figure 1C). Further analysis of fibroblasts isolated from uninjured and injured mice hearts demonstrated the expression of fibroblast markers (Periostin, Vimentin, Col1α1, or MEFSK4) and the absence of endothelial (CD31), hematopoietic (CD45), and pericyte (AN2/NG2) cell-specific markers (Figure S3), indicating a highly enriched fibroblast population without detectable contamination of other cell types. Previous studies indicate that cellular *Sprr3* expression can be induced
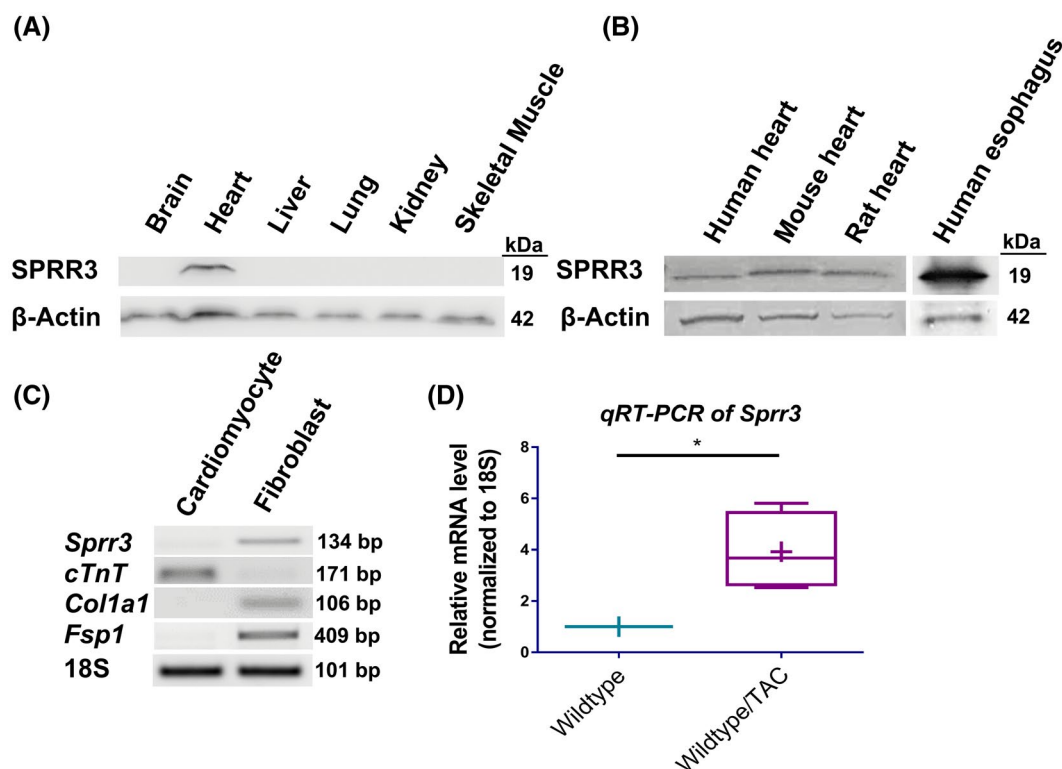
FIGURE 1 SPRR3 protein and transcripts are expressed only in fibroblasts in murine heart. A, Tissue extracts from mouse organs were probed with anti-SPRR3 antibody by western blot and showed detectable levels only in the heart. β-actin served as a loading control. B, Tissue extracts from human, mouse, and rat heart were assayed by western blot for SPRR3 and all showed presence of protein. Esophagus served as a positive control. C, cDNA from cardiomyocytes and cardiac fibroblasts isolated from wild-type mice were analyzed by RT-PCR for the presence of *Sprr3* and appropriate markers (*cTnT* for cardiomyocytes; *Fsp1* and *Col1a1* for fibroblasts). *Sprr3* transcript expression was only detected in the fibroblast population. A 18S served as a loading control. D, Hearts were isolated from wild-type mice that received either sham or TAC surgery and were assayed for *Sprr3* transcript levels by RT-PCR and normalized to 18S. Statistical analysis was performed by t test, where *$P < .05$, n = 4. For data presented as box-and-whiskers plots, horizontal lines indicate the medians, cross marks indicate the means, boxes indicate the 25th to 75th percentiles, and whiskers indicate the minimum and maximum values of the data set

by mechanical stress,[19] so we evaluated expression of *Sprr3* in freshly isolated cardiac fibroblasts 60 days after pressure overload in the TAC model. Consistent with our previous observations in smooth muscle cells,[11] we observed that following in vivo pressure overload stimulus, *Sprr3* transcript expression increased 4-fold in fibroblasts (Figure 1D). *Sprr3* expression was only detected in fibroblasts but not in cardiomyocytes and endothelial cells which were freshly isolated 60 days following TAC (Figure S4). These data indicate that cardiac fibroblasts are the major cells expressing *Sprr3* transcripts in the heart.

3.2 | *Sprr3* loss preserved mouse cardiac function from TAC

We previously developed a global *Sprr3* null mouse ($Sprr3^{-/-}$) to study the role of SPRR3 protein on atheroma burden.[21] We induced TAC to investigate the role of SPRR3 during pressure overload induced cardiac function and fibrosis in WT and $Sprr3^{-/-}$ mice. We compared percent change in echocardiography parameters at day 60 vs day 7 after TAC between $Sprr3^{-/-}$ and WT mice. We observed reduced left ventricular internal diameter end diastole (Δ LVIDd%; 8.6 ± 13, n = 14 vs -0.04 ± 0.4, n = 8, P = .042) and systole (Δ LVIDs%; 19 ± 21, n = 14 vs 3.8 ± 8, n = 8; P = .05) in $Sprr3^{-/-}$ mice, as well as increased ejection fraction (Δ EF%, -6.7 ± 6.1, n = 14 vs -2.1 ± 4.5, n = 8, P = .0240) (Table 2, Figure 2A). We did not observe any differences in cardiomyocyte size (868 ± 276 n = 100 vs 845 ± 295 n = 58, P = .6276) or heart weight to body weight ratios (6.927 ± 1.856, n = 9 vs 6.481 ± 1.103, n = 9; P = .5443) between wild-type and $Sprr3^{-/-}$ mice (Figure 2B,C). We did observe that loss of SPRR3 has protective effects in the TAC pressure-induced fibrosis/HF model in both preserving LV function and in reducing adverse remodeling.

3.3 | *Sprr3* loss reduced TAC-induced collagen type I deposition and fibroblast cell number in the heart

To determine if *Sprr3* loss protected against development of heart failure as reflected by echocardiography, we assessed both fibroblast numbers and collagen deposition in wild-type and $Sprr3^{-/-}$ hearts at day 60 after TAC. Fibroblast numbers were measured by IF staining with periostin, a marker of activated fibroblasts,[27] and collagen deposition was assessed by Masson's trichrome staining. Larger areas of interstitial and perivascular collagen deposition were detected in wild-type hearts (Figure 2D). Consistent with increased collagen deposition, we also observed significantly more periostin-positive cells in wild-type mouse vs $Sprr3^{-/-}$ hearts (52.60 ± 35.26, n = 10 vs 11.50 ± 8.689, n = 6; P = .0153) (Figure 2E,F).

Loss of *Sprr3* resulted in significant reduction of interstitial activated fibroblast numbers and matrix deposition/fibrosis.

3.4 | SPRR3 promotes both cell proliferation and collagen production in cardiac fibroblasts

As cardiac fibroblasts are the major source of collagen in the heart, we isolated them from digested mouse hearts and confirmed the fibroblast phenotype by demonstrating expression of type I collagen (red) by IF (Figure S1A). This cell population was negative for αSMA (green), indicating that it was comprised of fibroblasts exclusive of myofibroblasts or contaminated by smooth muscle cells. As expected, *Sprr3* mRNA and protein were detectable in the wild-type cells but not $Sprr3^{-/-}$ fibroblasts (Figure S1B). Real-time RT-PCR evaluation of freshly isolated fibroblasts from wild-type and $Sprr3^{-/-}$ hearts without TAC demonstrated lower levels of COL1A1 transcript in both $Sprr3^{-/-}$ and wild-type fibroblasts. Following TAC, these transcripts were nearly 3-fold higher in wild-type than $Sprr3^{-/-}$ fibroblasts (14.83 ± 0.29 vs 5.15 ± 0.65) (Figure 2G).

We previously reported that *Sprr3* regulates both type I collagen transcript and protein levels in vascular smooth muscle cells.[21] To determine if the increased numbers of cardiac fibroblasts in wild-type mice vs $Sprr3^{-/-}$ mice were elicited by increased proliferation vs survival, we performed proliferation and apoptosis assays on primary cardiac fibroblasts. Our data indicated that the presence of *Sprr3* increased fibroblast proliferation ($11\,863$ cells ± 240.8 vs 9445 cells ± 1035, P = .0169 following 48 hours of culture; seeding density 5000 cells/well) but had no effect on cell apoptosis (0.089 ± 0.039 vs 0.096 ± 0.032; P = .7530) (Figure 2H,I). Taken together, the decreased fibrosis observed in $Sprr3^{-/-}$ mice was the result of both decreased matrix synthesis by *Sprr3*-deficient fibroblasts as well as decreased fibroblast numbers due to their decreased proliferative capacity.

3.5 | *Sprr3*-dependent *Col1a1* expression in fibroblasts is related to Akt activation

We previously reported that regulation of type I collagen transcript levels by *Sprr3* may be PI3K/Akt dependent.[20,21] Other studies have also shown that Akt signaling can modulate type I collagen levels in various cell types.[28-30] We used mouse embryonic fibroblasts (MEFs) isolated from wild-type and $Sprr3^{-/-}$ mice to demonstrate that both pAKT levels and COL1A1 protein levels were significantly reduced in *Sprr3*-deficient cells with minimal change to total Akt levels (Figure 3A). When *Sprr3*-deficient cells were transiently transfected with a vector expressing human *SPRR3*

TABLE 2 SPRR3 loss results in reduced adverse cardiac remodeling and preserved mouse cardiac function from TAC (Day 7 to day 60). *Sprr3^{-/-}* mice showed significant improvement in cardiac ejection fraction (EF) and reduction in adverse cardiac remodeling measured by LVIDd and LVIDs

Echo parameters		WT mice	Sprr3^{-/-} mice	*P* values
LVIDD (mm)	D7	3.473 ± 0.47	3.454 ± 0.25	ns; *P* = .97
	D60	3.739 ± 0.35	3.437 ± 0.25	ns; *P* = .098
LVIDS (mm)	D7	1.916 ± 0.30	1.883 ± 0.23	ns; *P* = .98
	D60	2.249 ± 0.34	1.944 ± 0.17	*P* = .03
EF	D7	78.62 ± 4.29	78.85 ± 4.95	ns; *P* = .81
	D60	73.15 ± 3.35	77.03 ± 2.92	*P* = .019
FS%	D7	44.9 ± 3.16	45.61 ± 3.44	ns; *P* = .66
	D60	40.14 ± 3.59	43.46 ± 2.36	*P* = .019
ΔLVIDD%		8.637 ± 12.95	−0.4488 ± 4.072	*P* = .0421
ΔLVIDS%		19.16 ± 21.82	3.80 ± 8.02	*P* = .050
ΔEF%		−10.38 ± 9.81	−4.29 ± 8.00	*P* = .024
ΔFS%		−6.72 ± 6.13	−2.10 ± 4.51	ns; *P* = .069
N		14		8

Measured echo values

	LVIDD			
	D7		**D60**	
	WT	**SPRR3^{-/-}**	**WT**	**SPRR3^{-/-}**
	3.157	3.510	3.877	3.585
	3.076	3.748	3.368	3.680
	3.606	3.531	4.190	3.687
	3.361	3.443	3.483	3.395
	3.565	3.769	3.707	3.504
	3.280	3.314	3.823	3.483
	3.015	2.970	3.252	2.900
	2.988	3.350	3.280	3.260
	4.339		3.544	
	3.653		3.877	
	4.150		3.980	
	3.090		4.050	
	3.710		3.470	
	3.640		4.450	
Average	3.473	3.454	3.739	3.437

	LVIDS			
	D7		**D60**	
	WT	**SPRR3^{-/-}**	**WT**	**SPRR3^{-/-}**
	1.718	1.759	2.281	2.003
	1.704	2.288	1.908	2.180
	2.098	1.996	2.662	2.085
	1.793	1.820	2.064	1.847
	2.010	2.098	2.186	1.942

(Continues)

TABLE 2 (Contineud)

	LVIDS			
	D7		**D60**	
	WT	**SPRR3⁻/⁻**	**WT**	**SPRR3⁻/⁻**
	1.779	1.813	2.152	1.894
	1.636	1.570	1.854	1.610
	1.616	1.720	1.827	1.990
	2.478		2.085	
	2.091		2.275	
	2.580		2.500	
	1.630		2.650	
	1.840		2.030	
	1.850		3.010	
Average	1.916	1.883	2.249	1.944
	Ejection fraction			
	D7		**D60**	
	WT	**SPRR3⁻/⁻**	**WT**	**SPRR3⁻/⁻**
	78.263	82.131	72.679	76.293
	77.304	70.160	75.655	72.419
	73.691	75.618	66.615	75.470
	79.154	79.550	72.575	78.032
	75.758	76.333	72.687	76.848
	78.308	77.788	75.600	77.962
	78.547	83.800	75.399	82.800
	78.769	85.400	76.786	76.400
	74.255		73.035	
	74.713		72.883	
	74.700		74.100	
	84.200		70.300	
	86.800		78.500	
	86.200		67.300	
Average	78.619	78.847	73.151	77.028
	Fraction shortening%			
	D7		**D60**	
	WT	**SPRR3⁻/⁻**	**WT**	**SPRR3⁻/⁻**
	45.591	49.903	41.156	44.129
	44.592	38.949	43.347	40.775
	41.808	43.462	36.467	43.462
	46.667	47.140	40.741	45.600
	43.619	44.324	41.026	44.574
	45.756	45.287	43.695	45.614
	45.721	47.100	43.006	44.500
	45.909	48.700	44.306	39.000
	42.880		41.188	
	42.751		41.331	

T A B L E 2   (Continued)

	Fraction shortening%			
	D7		D60	
	WT	SPRR3$^{-/-}$	WT	SPRR3$^{-/-}$
	37.800		37.200	
	47.300		34.600	
	50.300		41.500	
	49.300		32.400	
Average	44.999	45.608	40.140	43.457

Note: Data presented in the top eight rows represent ± SD values for echo parameters at day 7 and day 30. In the bottom four rows, the data represent ± SD percent difference (Δ) between day 7 and day 60 for an average of n = 14 for WT mice and n = 8 for *Sprr3*$^{-/-}$ mice. All the measured echo values are presented separately (below). Statistical difference between cardiac parameters was determined by nonparametric Mann-Whitney test; $P < .05$ was considered significant.

cDNA, COL1A1 protein expression was significantly increased (Figure 3B), while the addition of a PI3K inhibitor, Ly294002, ablated this increase (Figure 3B). Moreover, transient transfection of *Sprr3*-deficient MEFs with vector expressing constitutively active *Akt* increased COL1A1 to levels similar to overexpression of *SPRR3* (Figure 3C). By contrast, cotransfecting both *SPRR3* cDNA and vector expressing dominant negative *Akt* reduced COL1A1 levels (Figure 3C). These data confirmed that *SPRR3* regulated collagen I expression through the PI3K/Akt pathway in *Sprr3*-deficient fibroblasts.

3.6 | SPRR3 loss affects Akt, FAK, and ERK signaling with no effects on TGFβ signaling

In addition to Akt signaling, FAK and ERK signaling have also been implicated in collagen deposition and turnover.[31,32] Deletion of fibroblast-specific FAK resulted in significant impairment in collagen synthesis.[32] In addition, gene expression of α1(I) and α2(I) collagen has been shown to be upregulated downstream of ERK signaling in normal as well as aberrant fibroproliferative conditions.[33,34] We assessed the effect of *Sprr3* loss on ERK and FAK signaling in parallel with its effects on Akt signaling and found that pFAK and pERK activation were significantly reduced in *Sprr3*$^{-/-}$ fibroblasts, similar to the effects on Akt activation (Figure 3D). TGF-β has also been reported to activate collagen production in fibroblasts. To understand whether SPRR3 has a connection with the TGFβ signaling pathway directly or through crosstalk of the PI3K/Akt pathway, we treated MEFs isolated from wild-type and *Sprr3*$^{-/-}$ mice with either PI3K/Akt inhibitors (Ly294002 and MK2206) or an activator (SC79). No difference in responsiveness to TGFβ was seen as assessed by pSMAD2 activation, and inhibitors for PI3K/Akt did not affect TGFβ pathway activity

(Figure S2). These data indicate that SPRR3 loss significantly reduced FAK and ERK signaling with no effect on the TGFβ signaling pathway directly or through crosstalk via the PI3K/Akt pathway.

3.7 | SPRR3 loss resulted in reduced PDGFRβ activation

The PDGFRβ pathway has been identified as being activated in cardiac fibroblasts following injury/fibrosis and it has been known to regulate PI3K/Akt signaling[35] and FAK.[36] We sought to determine whether SPRR3 was regulating these various signaling pathways via alterations in expression or activation of PDGFRβ. We did not observe any change in total PDGFRβ expression in *Sprr3*$^{-/-}$ cells (Figure 3E). However, both the rate and degree of activation of receptor phosphorylation were significantly reduced in *Sprr3*$^{-/-}$ as compared to WT fibroblasts when they were stimulated with recombinant PDGFBB and assessed at 2-minute intervals (Figure 3E). In order to assess if PDGFRβ in *Sprr3* deficient cells had diminished capacity to bind ligand, we used biotinylated recombinant PDGFBB at increasing concentrations and found that its receptor binding was not inhibited in SPRR3-deficient cells (Figure 3F). Taken together, although both ligand binding ability and expression levels of PDGFRβ were unchanged, *Sprr3*$^{-/-}$ cells had reduced capacity to activate PDGFRβ.

3.8 | Integrin β1 expression and integrin mediated cell functions are unaltered by *Sprr3* deletion

Integrin β1 has been reported to associate with PDGFRβ and coordinately alter the signaling pathways AKT, FAK, ERK, and p38.[37] The activation of FAK through integrin β1 has also

been implicated in pressure-overload mediated fibrosis.[11] We assessed integrin β1 cell surface expression as well as the activation of integrin β1 by flow cytometry. We found that there was no statistically significant difference in the number of cells expressing these integrins or the amount of integrin expressed per cell (mean fluorescence intensity) between wild-type and *Sprr3*^{−/−} fibroblasts (Figure 4A). Furthermore, we assessed integrin β1-dependent cell functions, including contraction, migration, and adhesion,[8] and found no differences between wild-type and *Sprr3*^{−/−} fibroblasts, consistent

with the lack of change in integrin expression or activation (Figure 4B-D).

3.9 | Integrin mediated activation of Akt, FAK, and p38 signaling was intact in *Sprr3*-deficient cells

To determine if FAK, Akt, and p38 could become activated in an integrin-adhesion-dependent manner in the absence of
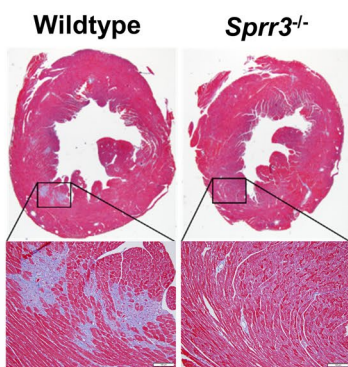

In vivo

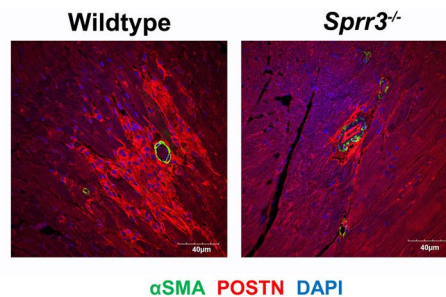(A) % LVIDd Change; % LVIDs Change; % EF Change

(B) Cardiomyocyte size

(C) Heart weight / Body weight

(D) Wildtype; Sprr3^{−/−}; Masson's Trichrome

(E) Wildtype; Sprr3^{−/−}; αSMA POSTN DAPI

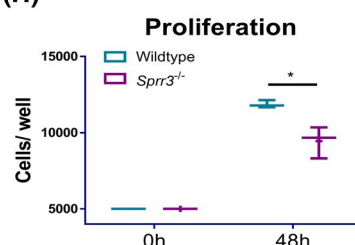(F) Cardiac Fibroblasts
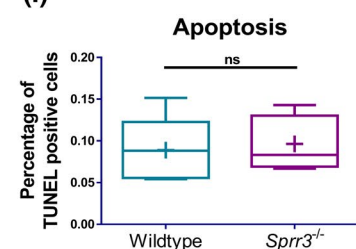
In vitro

(G) Col1a1

(H) Proliferation

(I) Apoptosis
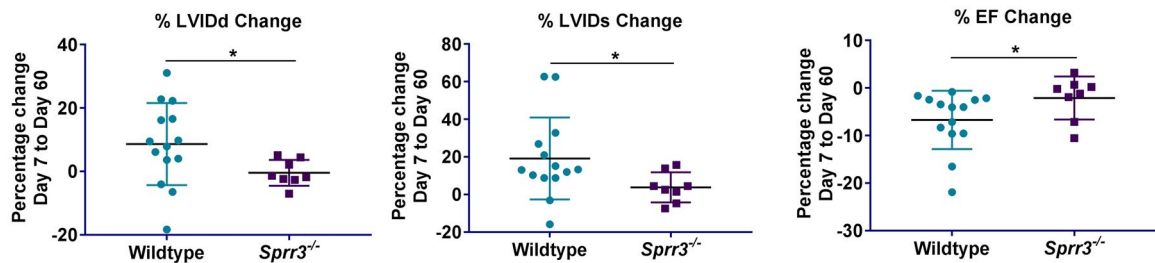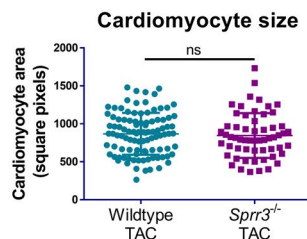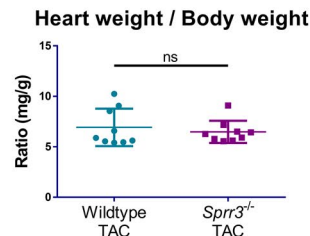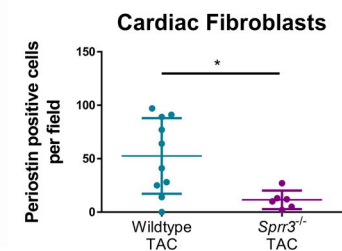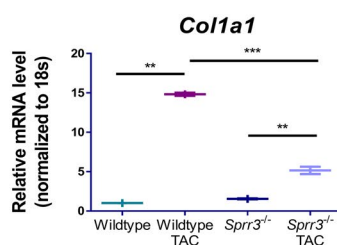
FIGURE 2 *Sprr3* loss preserved cardiac function from TAC and induced fibrosis by decreased fibroblast proliferation and collagen synthesis. A, Male wild-type (n = 14) and *Sprr3*$^{-/-}$ (n = 8) mice received TAC surgery at 3 months of age. Echocardiography analysis was performed at day 7 and day 60 after TAC. Data for left ventricular internal diameter end diastole (LVIDd), left ventricular internal diameter end systole (LVIDs) and ejection fraction (EF) were plotted as percentage difference between 7 and 60 days after TAC to reflect that presence of *Sprr3* led to worsening cardiac function. Statistical analysis was performed by Mann-Whitney test where *P < .05, **P < .01. For wild-type samples, n = 14, for *Sprr3*$^{-/-}$ samples, n = 8. B, Cardiomyocyte size was unchanged between genotypes. For wild-type n = 100; for *Sprr3*$^{-/-}$ n = 58. C, Heart weight vs body weight was quantified 60 days after TAC, n = 9. B and C, Statistical analysis was performed by two-tailed *t* test where ns = P > .05. D, Masson's trichrome staining of hearts from wild-type and *Sprr3*$^{-/-}$ mice was performed 60 days after TAC. Fibrotic area is indicated in blue by arrows, where wild-type hearts exhibit more fibrosis. Scale bars represent 100 μm. E, Confocal microscopy of immunofluorescent staining of heart tissue 60 days after TAC for anti-αSMA (green) and anti-periostin (red) was performed to identify fibroblasts. Scale bars represent 40 μm. F, Quantification of periostin positive cells per field indicates that wild-type hearts contain more activated fibroblasts. Statistical analysis was performed by *t* test where *P < .05, wild-type n = 10, *Sprr3*$^{-/-}$ n = 6. G, Levels of *Col1a1* were analyzed in cardiac fibroblasts (P1-P3) from wild-type and *Sprr3*$^{-/-}$ mice 60 days post sham or TAC surgery. Collagen transcripts were significantly elevated in both genotypes after TAC, but at a lower level in *Sprr3*$^{-/-}$ fibroblasts compared to wild-type. Statistical analysis was performed by one-way ANOVA with Bonferroni multiple comparisons analysis where *P < .05, **P < .01, ***P < .001, n = 3. H, Proliferation was measured using a DNA quantification kit after plating (0 hrs) or after 48 hours. Proliferation was lower in *Sprr3*$^{-/-}$ fibroblasts ((P1-P3), indicating that the reduced fibroblast numbers in vivo may be due to decreased proliferation rather than differing apoptosis levels. Statistical analysis was performed by *t* test only at 48 hours where *P < .05, n = 3. At 0 hours the same number of cells were plated, thus, no statistical test was performed. I, Apoptosis was analyzed by TUNEL staining (P1-P3). Statistical analysis was performed by *t* test where P > .05 (ns, not significant), n = 5. For data presented as box-and-whiskers plots, horizontal lines indicate the medians, cross marks indicate the means, boxes indicate the 25th to 75th percentiles, and whiskers indicate the minimum and maximum values of the data set

growth factors or serum, fibroblasts were plated on fibronectin-coated plates and collected at 15-minute intervals for up to 90 minutes.[38] All three molecules demonstrated increased activation compared to baseline (Figure 4F) to a similar degree at multiple time points, in both wild-type and *Sprr3*-deficient cells (Figure 4E), although total degree of activation was comparatively reduced in *Sprr3*-deficient cells. These results suggested that fibronectin mediated integrin ligation was intact in both WT and with SPRR3 loss and activated downstream signaling pathways, Akt, p38, and FAK, were observed in both wild-type and *Sprr3*$^{-/-}$ fibroblasts in the absence of growth factor/serum.

## 3.10 | SPRR3 interacts with PDGFRβ and integrin β1 and is necessary for their colocalization

It has been established that integrins and growth factors interact to facilitate signal transduction, although this synergistic process is not completely understood.[10] We assessed whether SPRR3 physically interacted with PDGFRβ or integrin β1 either directly or indirectly by co-immunoprecipitation (IP). *Sprr3*$^{-/-}$ cells were stably transduced with either GFP (control) or *Sprr3* cDNA. IP with antibodies to integrin β1, pulled down both SPRR3 and PDGFRβ in WT cells. By contrast, PDGFRβ was not pulled down from *Sprr3*-deficient cell-derived lysates. Conversely, PDGFRβ antibodies pulled down both integrin β1 and SPRR3 in wild-type cells, while

the antisera did not pull down significant levels of either protein in SPRR3-deficient lysates. These data suggested that SPRR3 is an important component or conduit to promote the interaction of PDGFRβ with integrin β1 (Figure 5A). To further verify these findings, we used in situ proximity ligation in which the secondary antibodies, which are conjugated to different oligonucleotides, are used to recognize distinct proteins using specific primary antibodies. If the oligonucleotides appended to the secondary antibodies are in close proximity (<16 nm), they can be ligated and be amplified through rolling circle PCR, then, tagged with a fluorescent probe, creating punctate staining that indicates physical proximity between two proteins.[39,40] In this case, fibroblasts were probed with integrin β1 and PDGFRβ primary antibodies and subsequently by oligonucleotide labeled respective secondary antibodies. Following completion of the steps of the assay (ie, PCR amplification, detection), the number of interactions per cell were quantified. *Sprr3*$^{-/-}$ fibroblasts had significantly fewer contacts between integrin β1 and PDGFRβ compared to the wild-type controls (25.18 ± 5.10 vs 7.524 ± 2.62, P < .0001) (Figure 5B). As a negative control, cells were incubated with the secondary antibodies in tandem. No significant fluorescence was observed in the negative control. Taken together, both immunoprecipitation and in situ ligation assays strongly suggest SPRR3 as an important protein that promotes the interaction between integrin β1 and PDGFRβ. To define if this interaction impacted cellular functions of SPRR3, we performed BrdU proliferation assays of WT and SPRR3-deficient MEFs in response to PDGFBB

treatment. PDGFBB had very minimal effects on proliferation of either WT or *Sprr3*-deficient MEFs. The addition of an antibody that ligates integrin β1 promoted proliferation of WT MEFs but not mutant MEFs in the presence of PDGFBB (Figure 5C). The observed increase in cell proliferation upon the co-activation of both integrin β1 and PDGFRβ in WT MEFs but not in *Sprr3*$^{-/-}$ MEFs further supported the important role of SPRR3 in the crosstalk of these two molecules for functional effects.

4 | DISCUSSION

The small proline rich repeat (SPRR) family of proteins are primarily known for their expression in epithelial cells where they are believed to play a role as protein-protein and protein-lipid linkers in the cornified epithelium.[41,42] Nonepithelial expression of several members, such as SPRR3 and SPRR2a, have been recently reported, yet their cellular and mechanistic roles are unclear.[22,23] Our group discovered high expression
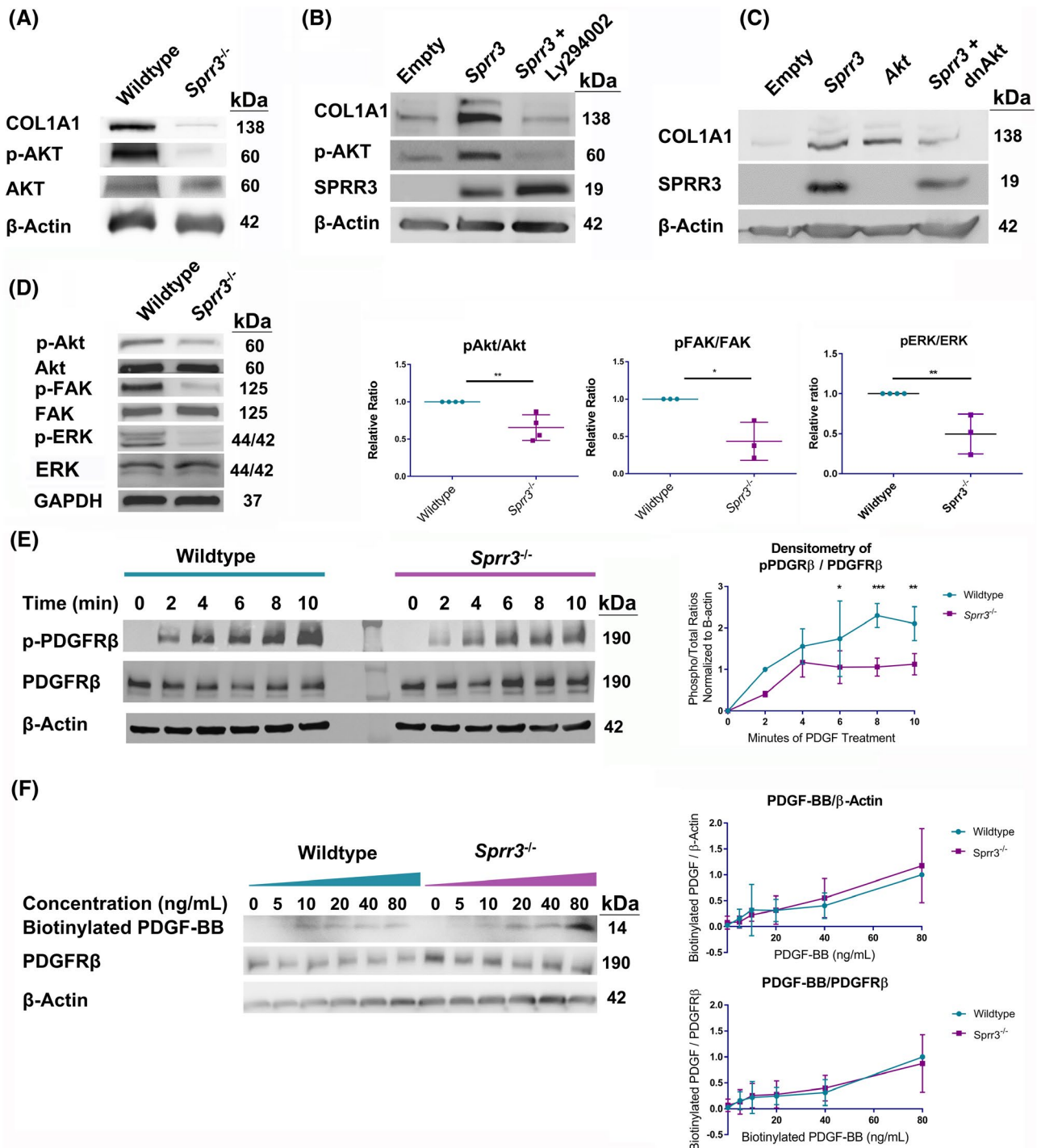
FIGURE 3 *Sprr3* upregulates collagen expression through the PI3K/Akt pathway and modulates PDGFRβ activation and downstream signaling. A, Mouse embryonic fibroblasts (MEFs; P1-P5) were analyzed by western blot for p-Akt, total Akt and type I collagen. Both collagen and activated Akt levels were reduced in *Sprr3*⁻/⁻ cardiac fibroblasts. β-actin served as a loading control. B, *Sprr3*⁻/⁻ MEFs were transfected with empty vector or vector expressing *Sprr3*. After 24 hours of transfection, cells were treated with or without PI3K inhibitor (Ly294002) for 24 hours. Cell lysates were probed for type I collagen, p-AKT, and SPRR3 by immunoblot. *Sprr3* expression could increase both activated AKT and collagen levels, but after AKT inhibition, levels of activated AKT and collagen were reduced to baseline. β-actin served as a loading control. C, *Sprr3*⁻/⁻ MEFs were transfected with empty vector or vector expressing *Sprr3*, *Akt* or dominant negative *Akt* (dnAkt). Protein was isolated 72 hours after transfection and probed for type I collagen and SPRR3. Collagen levels could be increased with either *Sprr3* or *Akt* expression alone but were not increased in cells expressing both *Sprr3* and dnAkt. β-actin served as a loading control. D, MEFs were serum starved for 4 hours and lysates were probed for p-Akt, total Akt, p-ERK, total ERK p-FAK, and total FAK by western analysis. Activated AKT and FAK were all reduced in *Sprr3*⁻/⁻ fibroblasts. GAPDH served as a loading control. Relative ratio of phosphorylated to total protein normalized to GAPDH is shown. Data were analyzed using a *t* test where *$P < .05$, **$P < .01$, n = 3-4. E, MEFs were serum starved and treated with recombinant PDGFBB at 2-minute intervals. Cell lysates were probed with p-PDGFRβ and total PDGFRβ by western blot and normalized to β-actin. Densitometry analysis of three independent experiments shows phosphorylated/total receptor levels normalized to β-actin. *Sprr3*⁻/⁻ fibroblasts were unable to activate PDGRB at similar levels to wild-type cells after 6 minutes of stimulation with PDGF. Data were analyzed using a 2-way ANOVA with repeated measures with a Sidak multiple comparisons test, where *$P < .05$, **$P < .01$, ***$P < .001$, n = 3. F, MEFs were serum starved then treated with biotinylated PDGFBB for 2 minutes at the indicated concentrations. Cell lysates were analyzed by western blot with antibodies against biotin or PDGRB. β-Actin served as a loading control. PDGFBB binding was unchanged between wild-type and *Sprr3*⁻/⁻ fibroblasts when normalized to either β-Actin or PDGFRβ levels. Statistical analysis was performed using a 2-way ANOVA with a Sidak multiple comparisons test, where $P > .05$, n = 3

of SPRR3 in atheromatous plaques of larger arteries where its expression is restricted to vascular smooth muscle cells.[20,21] In response to mechanical stress, SPRR3 upregulates type I collagen expression in VSMCs, augments proliferation, and enhances basal phosphorylation of Akt and p38.[19,20] In this study, we report that SPRR3 expression was detected in murine hearts (but not in other tested tissues such as brain, liver, lung, kidney or skeletal muscle), where its expression was restricted to another mesenchyme-derived cell type, the cardiac fibroblast. Similar to VSMCs, SPRR3 increased both type I collagen expression and cell proliferation. In cardiac fibroblasts, loss of SPRR3 reduced activation of several signaling pathways, such as FAK, Akt, ERK, and p38 as well as PDGFRβ in cardiac fibroblasts. The focus of our studies was to better elucidate SPRR3's molecular role in the diverse array of signaling molecules.

In order to study biomechanical stimulus-induced expression and function of SPRR3 in cardiac fibroblasts, we utilized the TAC injury model of pressure overload. Pressure overload in the heart can be caused by systemic hypertension and stenotic valvular heart diseases.[43] As a result, the heart adapts to maintain cardiac output through inducing cardiac hypertrophy, fibrosis, and inflammation,[43,44] where eventually this may lead to heart failure due to excessive hypertrophy and fibrosis.[45] Although *Sprr3* transcripts were detected in the adult murine heart at very low levels in cardiac fibroblasts at baseline, both protein and transcript levels increased significantly following TAC, suggesting that similar to its behavior in VSMCs, SPRR3 expression was regulated by mechanical stimulation.[19,20] Loss of *Sprr3* reduced fibrosis (interstitial matrix deposition), fibroblast density, and ameliorated parameters of heart failure. Additionally, we found that *Sprr3* loss resulted in reduced proliferation, reduced type

I collagen transcript and protein synthesis in isolated cardiac fibroblasts. Our in vitro findings were consistent with the in vivo protective observations resulting from *Sprr3* loss in a pressure-induced fibrosis/HF model. Although we are working with a global *Sprr3* KO model, we are confident that our findings are not due to an effect on VSMCs or an indirect effect via impact on vasculature. Briefly, we have published data[19,20] that there were no histologic differences in various tissues of KO vs WT mice (liver, heart, kidney, and lung). We evaluated large arteries, veins, smaller vessels, and capillaries and found no histologic differences, specifically there were no differences in cellular organization or cell numbers/medial thickness of vessels in uninjured WT and *Sprr3* KO mice. There were also no differences in blood pressure between WT and *Sprr3* KO animals (data not shown). We also evaluated endothelial cells isolated from large vessels and identified no difference in in vitro functional parameters (proliferation, migration, and network formation). We have looked at the lifespan of WT vs *Sprr3* KO mice and identified no differences. Further to confirm SPRR3 expression in fibroblasts and not in other cell types, we isolated fibroblasts, cardiomyocytes, and endothelial cells following TAC and identified SPRR3 expression only in fibroblasts. SPRR3 transcripts were not identified in endothelial cells or cardiomyocyte in mouse hearts following TAC. Furthermore, our molecular and phenotype analysis of the isolated fibroblasts indicate that there was no detectable contamination with VSMCs or pericytes.

Previously, our lab identified that *Sprr3* expression itself is regulated by transduction of biomechanical stress involving integrin α1β1 binding to collagen in VSMCs.[19] Integrins serve as the major family of extracellular matrix receptors in many cell types, including cardiac fibroblasts.[46] Relevant

to this study of cardiac fibroblasts, integrin β1 has been implicated in cardiac fibroblast activity, including adhesion, migration, and other cellular behavior, via interaction with extracellular matrix.[8,47] Moreover, fibroblasts respond to mechanical loading by increasing matrix synthesis, which

can contribute to fibrosis.[48-50] FAK, a signaling molecule downstream from integrins, has been shown to play a role in the activation of cardiac fibroblasts and development of fibrosis[51] and inhibition of FAK resulted in attenuated fibrosis and collagen content in pressure overload.[11,52] It
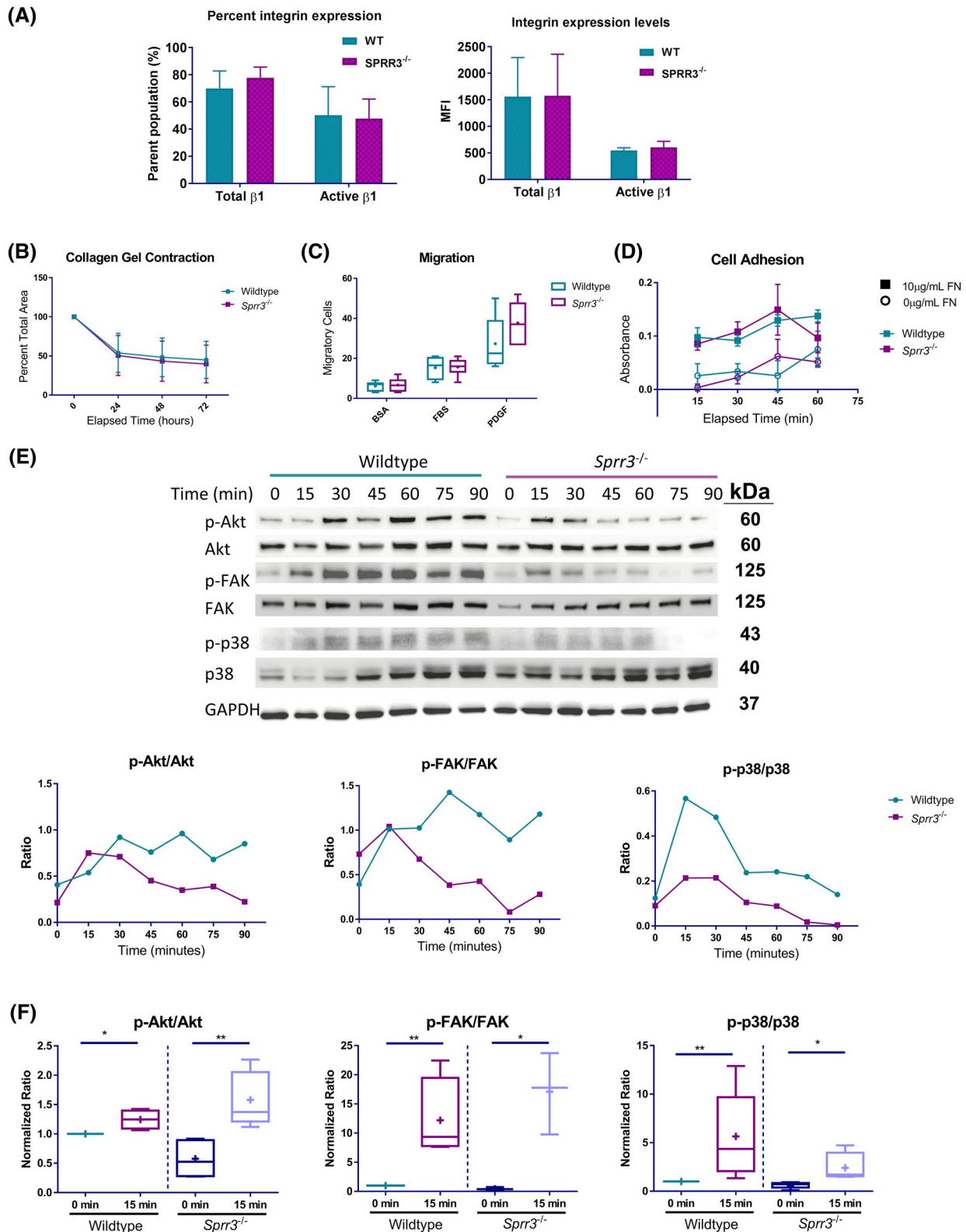
FIGURE 4 Integrin β1 levels, activation and mediated cell activity are not modulated by Sprr3, but downstream signaling activation is impaired in $Sprr3^{-/-}$ fibroblasts. A, Flow cytometry analysis of integrin β1 (total and active conformation) in wild-type and $Sprr3^{-/-}$ MEFs (P1) show no differences in percentage of cell expression or mean fluorescence intensity (MFI). Statistical analysis was performed by 2-way ANOVA with Sidak multiple comparisons test, $^{ns}P > .05$, n = 3. B, MEFs (P1-P5) were serum starved and plated within a collagen gel and allowed to contract the gel over 72 hours. Data are presented in percentage of total area, where no differences were observed between genotypes. Statistical analysis was performed by 2-way ANOVA with repeated measures and a Sidak multiple comparisons test, $P > .05$, n = 12. C, MEFs (P1-P5) were serum starved then plated in transwells to perform a Boyden's chamber assay. Membranes were coated with BSA (negative control) or fibronectin. FBS or PDGF was placed in media in the bottom well as a stimulus. No differences were detected in any condition. Statistical analysis was performed by t test where $^{ns}P > .05$, n = 6. D, MEFs (P1-P5) were serum starved then plated on 10 μg/mL or 0 μg/mL (negative control) fibronectin (FN) at 15-minute intervals to determine cell adhesion. Crystal violet stained cells were quantified by absorbance, and no differences were noted between genotypes. Statistical analysis was performed by 2-way ANOVA with Sidak multiple comparisons test, $^{ns}P > .05$, n = 3. E, MEFs (P1-P5) were serum starved, then, plated on 1 μg/mL fibronectin coated plates at 15-minute intervals in serum-free media. Lysates were analyzed by western blot for phosphorylated and total Akt, FAK and p38, then, normalized to GAPDH loading control. Densitometry analysis of normalized ratios is presented in the graphs. Densitometry over time is n = 1 for all timepoints. Differences between 0 and 15 minutes were performed by t test where $*P < .05$, $**P < .01$, n = 3-7

is also recognized that integrins, which transduce signals from the extracellular matrix, act coordinately with growth factor receptors to optimize signal transduction.[10] Many of the cellular signals activated by integrins, including FAK activation, are also elicited by PDGF receptor beta activation.[53-55] Both PDGF growth factor and PDGF receptors (PDGFRs) are upregulated following myocardial injury, specifically in cardiac fibroblasts and myofibroblasts.[56] PDGF growth factors significantly stimulate cardiac fibroblast proliferation in vitro, and neutralization of PDGF receptors alpha and beta reduces collagen deposition in the myocardium in vivo.[57] Additionally, overexpression of PDGFRβ in cardiac fibroblasts leads to enhanced proliferation and collagen synthesis.[58,59] In addition to downregulation of several downstream signaling molecules, such as FAK, p38, and ERK, we found that $Sprr3$ loss resulted in significantly reduced activation of PDGFRβ following stimulation with PDGFBB, although neither the expression of PDGFRβ nor binding of PDGFBB to its receptors were notably different in $Sprr3$ deficient cells as compared to controls.

There are numerous studies that have demonstrated integrin mediated signaling often overlaps with growth factor receptor signaling pathways, including MAPK, FAK, PI3K-Akt, and Rho family GTPases.[10,60-62] Evidence of cooperative signaling specifically between integrin β1 and PDGFRβ that demonstrated activation of integrin β1 can result in the activation and downstream signaling via PDGFRβ was published 20 years ago.[10] However, the structural basis of this interaction is still not well understood.[10] The support for our hypothesis that SPRR3 may be physically modulating integrin β1 and growth factor coordinate signaling was provided by our co-immunoprecipitation studies where we demonstrated that the absence of SPRR3 resulted in

significantly diminished association of PDGFRβ and integrin β1 in reciprocal immunoprecipitation experiments. This was further confirmed by in situ proximity ligation experiments, indicating that without SPRR3, the physical interactions between these receptors were greatly diminished. Consequently, our studies supported that SPRR3 enhanced the physical association and signaling crosstalk between PDGFRβ and integrin β1. By facilitating this crosstalk, we propose a model in which SPRR3 is a conduit in the transduction of biomechanical and other matrix-related signals with growth factor signaling. We are aware of one other example, in which a small protein known for its role in cross-linking proteins, the cell-surface transglutaminase, was found to regulate PDGFR/integrin association, downstream cooperative signaling, and cell behavior.[63] Furthermore, enhanced proliferation of $Sprr3$ expressing fibroblasts in the presence of integrin β1 cross-linking antibody identified the functional significance of integrin β1 and SPRR3 interaction.

The SPRR family of proteins all have similar structure which consists of amino- and carboxyl-terminal domains, which comprise of several glutamine and lysine residues, with a central repetitive proline-rich domain.[64] The SPRR proteins have highly specific expression patterns that are differentially regulated during development.[65-67] In disease, SPRR expression changes have been reported in keratinization and skin inflammatory disorders,[68] as well as in a wide array of cancers and cancer cell lines.[69] Based on the data presented in this paper which suggested SPRR3 modulated integrin and growth factor association and signaling, it is possible that other members of the SPRR family may perform similar roles, albeit with different molecular specificities, in biomechanical signal transduction.
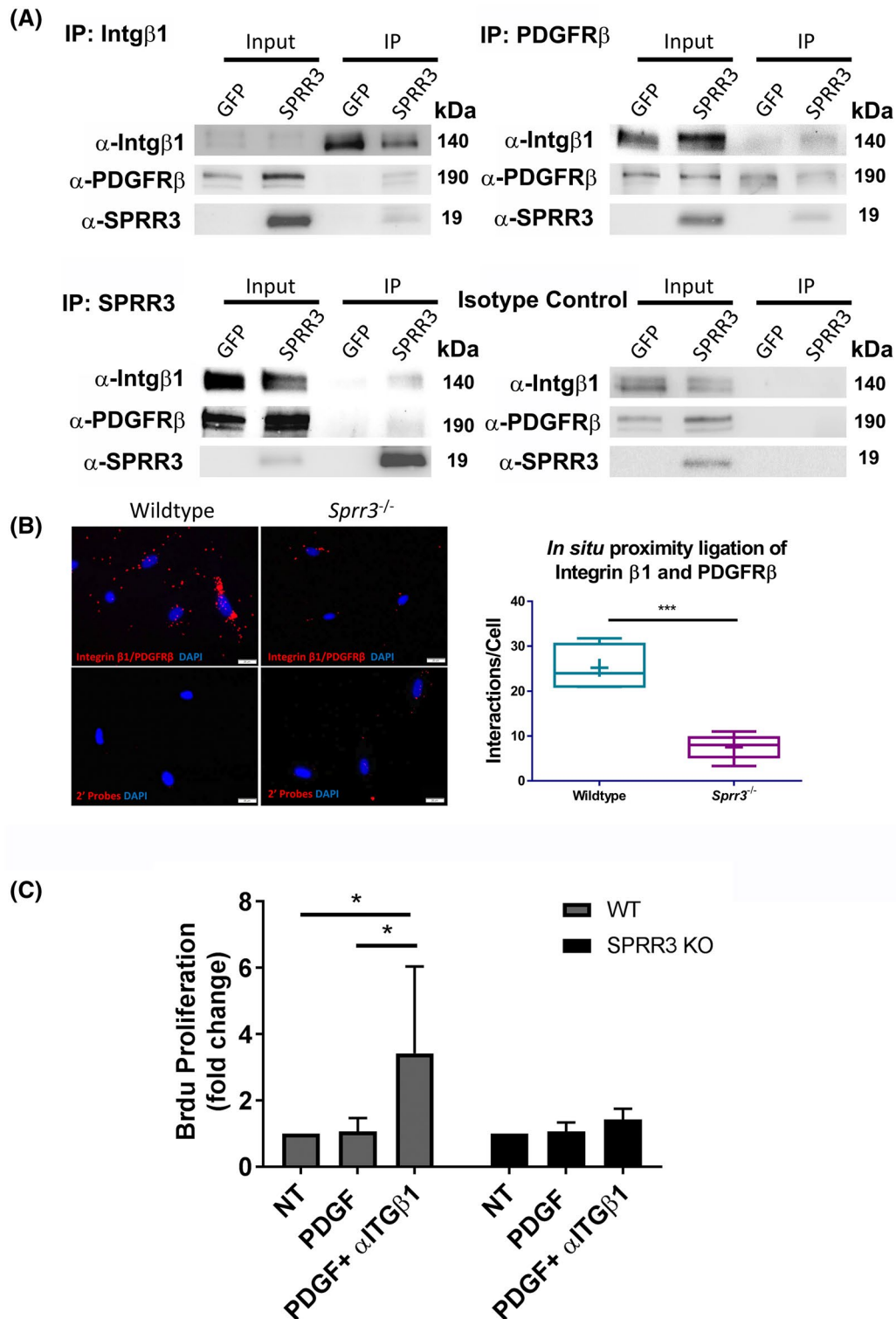
FIGURE 5 SPRR3 interacts with PDGFRβ and integrin β1 and facilitates their interaction. A, *Sprr3*$^{-/-}$ MEFs (P1-P5) overexpressing either GFP or SPRR3 were used for immunoprecipitation (IP) of PDGFRβ, integrin β1 and SPRR3. Western blot analysis of the input cell lysates and IP eluate are shown. IP of PDGRβ was able to pull down integrin β1 only in the presence of SPRR3, as well as SPRR3 itself. Conversely, IP of integrin β1 was only able to pull-down PDGFRβ in the presence of SPRR3, as well as SPRR3. SPRR3 pull-down identified both integrin β1 and PDGFRβ in cells positive for SPRR3 (not GFP knockout cells). Negative isotype controls did not display any of the proteins after pull-down. B, In situ proximity ligation of Integrin β1 and PDGFRβ showed enhanced receptor pairs in wild-type MEFs compared to *Sprr3*$^{-/-}$ MEFs (indicated by red). Secondary probes showed minimal staining. Scale bars represent 20 μm. Average interactions per cell (indicated by DAPI stain) per field were quantified. Statistical analysis was performed by *t* test where ***$P < .001$, n = 4-7. C, WT and *Sprr3*$^{-/-}$ MEFs (P1-P5) were serum starved, then, plated on 1 μg/mL fibronectin coated plates in serum-free media for 24 hours. Cells were treated with/without 10 μg/mL Integrin β1 antibody for 1 hour at 37°C prior to stimulation with PDGF. BrdU labeling was done for 18 hours and BrdU proliferation assay was performed as per manufacturer's instructions (Millipore). Statistical analysis was performed using a 2-way ANOVA, where $P < .05$, n = 3
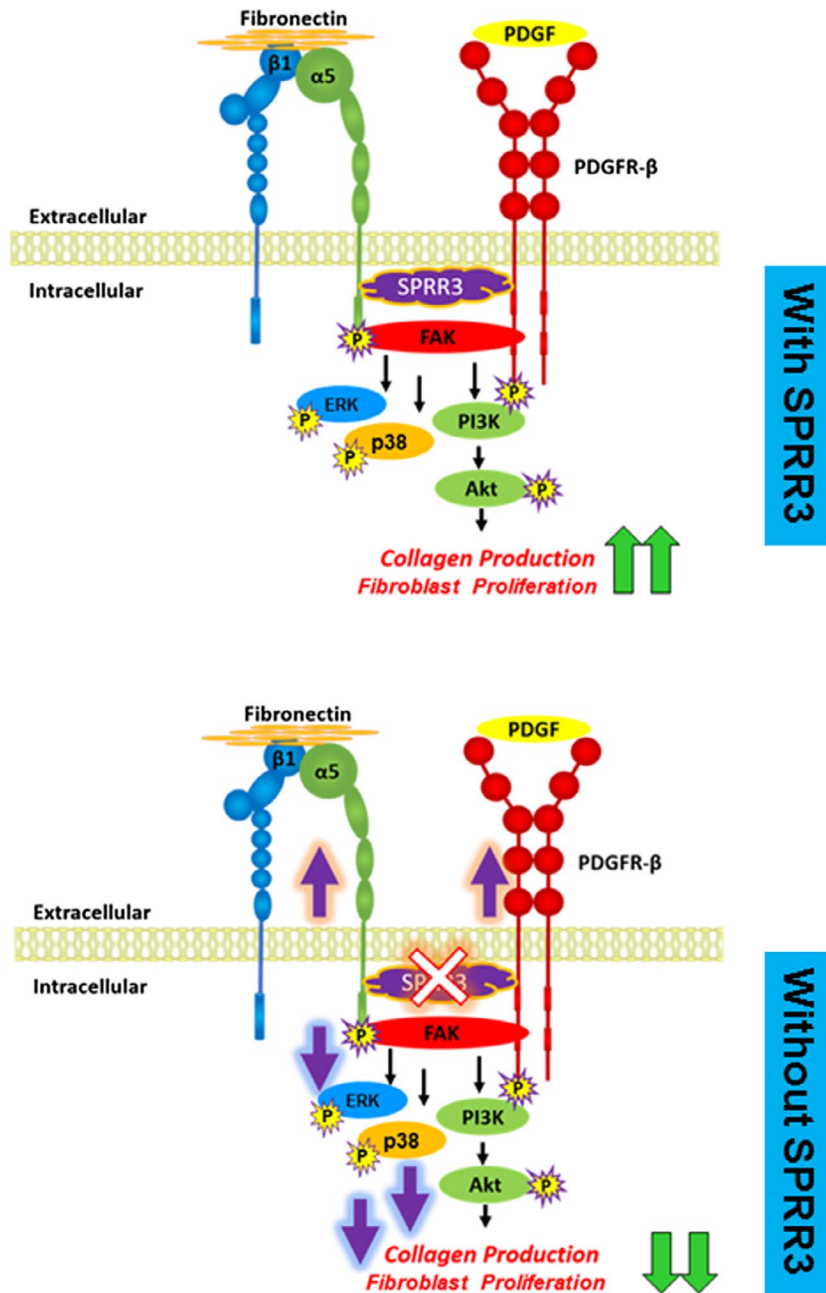
FIGURE 6 A model depicting the function of SPRR3 in modulating growth factor mediated signaling to promote collagen production. SPRR3 facilitates the coordinated activation of Integrin β1 and PDGFRβ to activate shared signaling pathways such as ERK, FAK, and AKT pathways. This harmonized augmentation of growth factor mediated signals with mechano-signals mediated by integrin β1 promotes fibroblast proliferation and the synthesis of collagen in fibroblasts. Model figure is adapted from Veevers-Lowe et al[70]

CONFLICT OF INTEREST

The authors declare no conflict of interest.

AUTHOR CONTRIBUTIONS

P.P. Young, R. Zent, S. Mathew, C.D. Lietman, and S. Saraswati designed research; C.D. Lietman, B. Li, and S. Saraswati performed research and analyzed data; P.P. Young, D. Lietman, and S. Saraswati wrote the paper.

ORCID

Sarika Saraswati (iD) https://orcid.org/0000-0002-5674-8371

REFERENCES

1. Valiente-Alandi I, Potter SJ, Salvador AM, et al. Inhibiting fibronectin attenuates fibrosis and improves cardiac function in a model of heart failure. *Circulation*. 2018;138:1236–1252.

2. Camelliti P, Borg TK, Kohl P. Structural and functional characterisation of cardiac fibroblasts. *Cardiovasc Res*. 2005;65:40-51.

3. Travers JG, Kamal FA, Robbins J, Yutzey KE, Blaxall BC. Cardiac fibrosis: The fibroblast awakens. *Circ Res*. 2016;118:1021-1040.

4. Souders CA, Bowers SL, Baudino TA. Cardiac fibroblast: The renaissance cell. *Circ Res*. 2009;105:1164-1176.

5. Souders CA, Borg TK, Banerjee I, Baudino TA. Pressure overload induces early morphological changes in the heart. *Am J Pathol*. 2012;181:1226-1235.

6. Banerjee I, Yekkala K, Borg TK, Baudino TA. Dynamic interactions between myocytes, fibroblasts, and extracellular matrix. *Ann N Y Acad Sci*. 2006;1080:76-84.

7. Holmes JW, Borg TK, Covell JW. Structure and mechanics of healing myocardial infarcts. *Annu Rev Biomed Eng*. 2005;7:223-253.

8. Stewart JA Jr, Massey EP, Fix C, Zhu J, Goldsmith EC, Carver W. Temporal alterations in cardiac fibroblast function following induction of pressure overload. *Cell Tissue Res*. 2010;340:117-126.

9. Babbitt CJ, Shai SY, Harpf AE, Pham CG, Ross RS. Modulation of integrins and integrin signaling molecules in the pressure-loaded murine ventricle. *Histochem Cell Biol*. 2002;118:431-439.

10. Ivaska J, Heino J. Cooperation between integrins and growth factor receptors in signaling and endocytosis. *Annu Rev Cell Dev Biol*. 2011;27:291-320.

11. Manso AM, Kang SM, Plotnikov SV, et al. Cardiac fibroblasts require focal adhesion kinase for normal proliferation and migration. *Am J Physiol Heart Circ Physiol*. 2009;296:H627-H638.

12. Aplin AE, Stewart SA, Assoian RK, Juliano RL. Integrin-mediated adhesion regulates ERK nuclear translocation and phosphorylation of Elk-1. *J Cell Biol*. 2001;153:273-282.

13. Moro L, Venturino M, Bozzo C, et al. Integrins induce activation of EGF receptor: role in MAP kinase induction and adhesion-dependent cell survival. *EMBO J*. 1998;17:6622-6632.

14. Sundberg C, Rubin K. Stimulation of beta1 integrins on fibroblasts induces PDGF independent tyrosine phosphorylation of PDGF beta-receptors. *J Cell Biol*. 1996;132:741-752.

15. Takada Y, Takada YK, Fujita M. Crosstalk between insulin-like growth factor (IGF) receptor and integrins through direct integrin binding to IGF1. *Cytokine Growth Factor Rev*. 2017;34:67-72.

16. Hohl D, de Viragh PA, Amiguet-Barras F, Gibbs S, Backendorf C, Huber M. The small proline-rich proteins constitute a multigene family of differentially regulated cornified cell envelope precursor proteins. *J Invest Dermatol*. 1995;104:902-909.

17. Gibbs S, Fijneman R, Wiegant J, van Kessel AG, van de Putte P, Backendorf C. Molecular characterization and evolution of the SPRR family of keratinocyte differentiation markers encoding small proline-rich proteins. *Genomics*. 1993;16:630-637.

18. Young PP, Modur V, Teleron AA, Ladenson JH. Enrichment of genes in the aortic intima that are associated with stratified epithelium: Implications of underlying biomechanical and barrier properties of the arterial intima. *Circulation*. 2005;111:2382-2390.

19. Pyle AL, Atkinson JB, Pozzi A, et al. Regulation of the atheroma-enriched protein, SPRR3, in vascular smooth muscle cells through cyclic strain is dependent on integrin alpha1beta1/collagen interaction. *Am J Pathol*. 2008;173:1577-1588.

20. Lietman CD, Segedy AK, Li B, et al. Loss of SPRR3 in ApoE$^{-/-}$ mice leads to atheroma vulnerability through Akt dependent and independent effects in VSMCs. *PLoS ONE*. 2017;12:e0184620.

21. Segedy AK, Pyle AL, Li B, et al. Identification of small proline-rich repeat protein 3 as a novel atheroprotective factor that promotes adaptive Akt signaling in vascular smooth muscle cells. *Arterioscler Thromb Vasc Biol*. 2014;34:2527-2536.

22. Kim JC, Yu JH, Cho YK, et al. Expression of SPRR3 is associated with tumor cell proliferation in less advanced stages of breast cancer. *Breast Cancer Res Treat*. 2012;133:909-916.

23. Cho DH, Jo YK, Roh SA, et al. Upregulation of SPRR3 promotes colorectal tumorigenesis. *Mol Med*. 2010;16:271-277.

24. Kong P, Christia P, Saxena A, Su Y, Frangogiannis NG. Lack of specificity of fibroblast-specific protein 1 in cardiac remodeling and fibrosis. *Am J Physiol Heart Circ Physiol*. 2013;305:H1363-H1372.

25. Chapman D, Weber KT, Eghbali M. Regulation of fibrillar collagen types I and III and basement membrane type IV collagen gene expression in pressure overloaded rat myocardium. *Circ Res*. 1990;67:787-794.

26. Strutz F, Okada H, Lo CW, et al. Identification and characterization of a fibroblast marker: FSP1. *J Cell Biol*. 1995;130:393-405.

27. Snider P, Standley KN, Wang J, Azhar M, Doetschman T, Conway SJ. Origin of cardiac fibroblasts and the role of periostin. *Circ Res*. 2009;105:934-947.

28. Yokoyama K, Kimoto K, Itoh Y, et al. The PI3K/Akt pathway mediates the expression of type I collagen induced by TGF-beta2 in human retinal pigment epithelial cells. *Graefes Arch Clin Exp Ophthalmol*. 2012;250:15-23.

29. Runyan CE, Schnaper HW, Poncelet AC. The phosphatidylinositol 3-kinase/Akt pathway enhances Smad3-stimulated mesangial cell collagen I expression in response to transforming growth factor-beta1. *J Biol Chem*. 2004;279:2632-2639.

30. Abeyrathna P, Su Y. The critical role of Akt in cardiovascular function. *Vascul Pharmacol*. 2015;74:38-48.

31. Hayashida T, Poncelet AC, Hubchak SC, Schnaper HW. TGF-beta1 activates MAP kinase in human mesangial cells: A possible role in collagen expression. *Kidney Int*. 1999;56:1710-1720.

32. Rajshankar D, Wang Y, McCulloch CA. Osteogenesis requires FAK-dependent collagen synthesis by fibroblasts and osteoblasts. *FASEB J*. 2017;31:937-953.

33. Palcy S, Goltzman D. Protein kinase signalling pathways involved in the up-regulation of the rat alpha1(I) collagen gene by transforming growth factor beta1 and bone morphogenetic protein 2 in osteoblastic cells. *Biochem J*. 1999;343(Pt 1):21-27.

34. Svegliati-Baroni G, Ridolfi F, Di Sario A, et al. Intracellular signaling pathways involved in acetaldehyde-induced collagen and fibronectin gene expression in human hepatic stellate cells. *Hepatology*. 2001;33:1130-1140.

35. Sadoshima J, Jahn L, Takahashi T, Kulik TJ, Izumo S. Molecular characterization of the stretch-induced adaptation of cultured cardiac cells. An in vitro model of load-induced cardiac hypertrophy. *J Biol Chem*. 1992;267:10551-10560.

36. Borkham-Kamphorst E, Weiskirchen R. The PDGF system and its antagonists in liver fibrosis. *Cytokine Growth Factor Rev*. 2016;28:53-61.

37. Moreno-Layseca P, Streuli CH. Signalling pathways linking integrins with cell cycle progression. *Matrix Biol*. 2014;34:144-153.

38. Bitterman P, Rennard S, Adelberg S, Crystal RG. Role of fibronectin in fibrotic lung disease. A growth factor for human lung fibroblasts. *Chest*. 1983;83:96S.

39. Bellucci A, Fiorentini C, Zaltieri M, Missale C, Spano P. The "in situ" proximity ligation assay to probe protein-protein interactions in intact tissues. *Methods Mol Biol*. 2014;1174:397-405.

40. Soderberg O, Leuchowius KJ, Gullberg M, et al. Characterizing proteins and their interactions in cells and tissues using the in situ proximity ligation assay. *Methods*. 2008;45:227-232.

41. Fischer DF, Sark MW, Lehtola MM, Gibbs S, van de Putte P, Backendorf C. Structure and evolution of the human SPRR3 gene: implications for function and regulation. *Genomics*. 1999;55:88-99.

42. Marenholz I, Zirra M, Fischer DF, Backendorf C, Ziegler A, Mischke D. Identification of human epidermal differentiation complex (EDC)-encoded genes by subtractive hybridization of entire YACs to a gridded keratinocyte cDNA library. *Genome Res*. 2001;11:341-355.

43. Oka T, Akazawa H, Naito AT, Komuro I. Angiogenesis and cardiac hypertrophy: Maintenance of cardiac function and causative roles in heart failure. *Circ Res*. 2014;114:565-571.

44. Baudino TA, Carver W, Giles W, Borg TK. Cardiac fibroblasts: Friend or foe? *Am J Physiol Heart Circ Physiol*. 2006;291:H1015-H1026.

45. Gulati A, Jabbour A, Ismail TF, et al. Association of fibrosis with mortality and sudden cardiac death in patients with nonischemic dilated cardiomyopathy. *JAMA*. 2013;309:896-908.

46. Terracio L, Rubin K, Gullberg D, et al. Expression of collagen binding integrins during cardiac development and hypertrophy. *Circ Res*. 1991;68:734-744.

47. Schluter KD, Wollert KC. Synchronization and integration of multiple hypertrophic pathways in the heart. *Cardiovasc Res*. 2004;63:367-372.

48. Berk BC, Fujiwara K, Lehoux S. ECM remodeling in hypertensive heart disease. *J Clin Investig*. 2007;117:568-575.

49. Frangogiannis NG. Matricellular proteins in cardiac adaptation and disease. *Physiol Rev*. 2012;92:635-688.

50. Chen C, Li R, Ross RS, Manso AM. Integrins and integrin-related proteins in cardiac fibrosis. *J Mol Cell Cardiol*. 2016;93:162-174.

51. Dalla Costa AP, Clemente CF, Carvalho HF, Carvalheira JB, Nadruz W Jr, Franchini KG. FAK mediates the activation of cardiac fibroblasts induced by mechanical stress through regulation of the mTOR complex. *Cardiovasc Res*. 2010;86:421-431.

52. Clemente CF, Tornatore TF, Theizen TH, et al. Targeting focal adhesion kinase with small interfering RNA prevents and reverses load-induced cardiac hypertrophy in mice. *Circ Res*. 2007;101:1339-1348.

53. Bornfeldt KE, Raines EW, Nakano T, Graves LM, Krebs EG, Ross R. Insulin-like growth factor-I and platelet-derived growth factor-BB induce directed migration of human arterial smooth muscle cells via signaling pathways that are distinct from those of proliferation. *J Clin Investig*. 1994;93:1266-1274.

54. Claesson-Welsh L. Platelet-derived growth factor receptor signals. *J Biol Chem*. 1994;269:32023-32026.

55. Williams LT. Signal transduction by the platelet-derived growth factor receptor. *Science*. 1989;243:1564-1570.

56. Fan B, Ma L, Li Q, Wang L, Zhou J, Wu J. Role of PDGFs/PDGFRs signaling pathway in myocardial fibrosis of DOCA/salt hypertensive rats. *Int J Clin Exp Pathol*. 2014;7:16-27.

57. Gallini R, Lindblom P, Bondjers C, Betsholtz C, Andrae J. PDGF-A and PDGF-B induces cardiac fibrosis in transgenic mice. *Exp Cell Res*. 2016;349:282-290.

58. Wang L, Ma L, Fan H, Yang Z, Li L, Wang H. MicroRNA-9 regulates cardiac fibrosis by targeting PDGFR-beta in rats. *J Physiol Biochem*. 2016;72:213-223.

59. Fan H, Ma L, Fan B, Wu J, Yang Z, Wang L. Role of PDGFR-beta/PI3K/AKT signaling pathway in PDGF-BB induced myocardial fibrosis in rats. *Am J Transl Res*. 2014;6:714-723.

60. Cabodi S, Moro L, Bergatto E, et al. Integrin regulation of epidermal growth factor (EGF) receptor and of EGF-dependent responses. *Biochem Soc Trans*. 2004;32:438-442.

61. Giancotti FG, Tarone G. Positional control of cell fate through joint integrin/receptor protein kinase signaling. *Annu Rev Cell Dev Biol*. 2003;19:173-206.

62. Schwartz MA, Ginsberg MH. Networks and crosstalk: Integrin signalling spreads. *Nat Cell Biol*. 2002;4:E65-E68.

63. Zemskov EA, Loukinova E, Mikhailenko I, Coleman RA, Strickland DK, Belkin AM. Regulation of platelet-derived growth factor receptor function by integrin-associated cell surface transglutaminase. *J Biol Chem*. 2009;284:16693-16703.

64. Backendorf C, Hohl D. A common origin for cornified envelope proteins? *Nat Genet*. 1992;2:91.

65. Fischer DF, Backendorf C. Identification of regulatory elements by gene family footprinting and in vivo analysis. *Adv Biochem Eng Biotechnol*. 2007;104:37-64.

66. Fischer DF, Gibbs S, van De Putte P, Backendorf C. Interdependent transcription control elements regulate the expression of the SPRR2A gene during keratinocyte terminal differentiation. *Mol Cell Biol*. 1996;16:5365-5374.

67. Yaar M, Eller MS, Bhawan J, Harkness DD, DiBenedetto PJ, Gilchrest BA. In vivo and in vitro SPRR1 gene expression in normal and malignant keratinocytes. *Exp Cell Res*. 1995;217:217-226.

68. Koizumi H, Kartasova T, Tanaka H, Ohkawara A, Kuroki T. Differentiation-associated localization of small proline-rich protein in normal and diseased human skin. *Br J Dermatol*. 1996;134:686-692.

69. Carregaro F, Stefanini AC, Henrique T, Tajara EH. Study of small proline-rich proteins (SPRRs) in health and disease: A review of the literature. *Arch Dermatol Res*. 2013;305:857-866.

70. Veevers-Lowe J, Ball SG, Shuttleworth A, Kielty CM. Mesenchymal stem cell migration is regulated by fibronectin through alpha5beta1-integrin-mediated activation of PDGFR-beta and potentiation of growth factor signals. *J Cell Sci*. 2011;124:1288-1300.

SUPPORTING INFORMATION

Additional Supporting Information may be found online in the Supporting Information section.